

Electronic supplementary information

Nanofibrous silicon/carbon composite sheet derived from cellulose substance as free-standing lithium-ion battery anodes

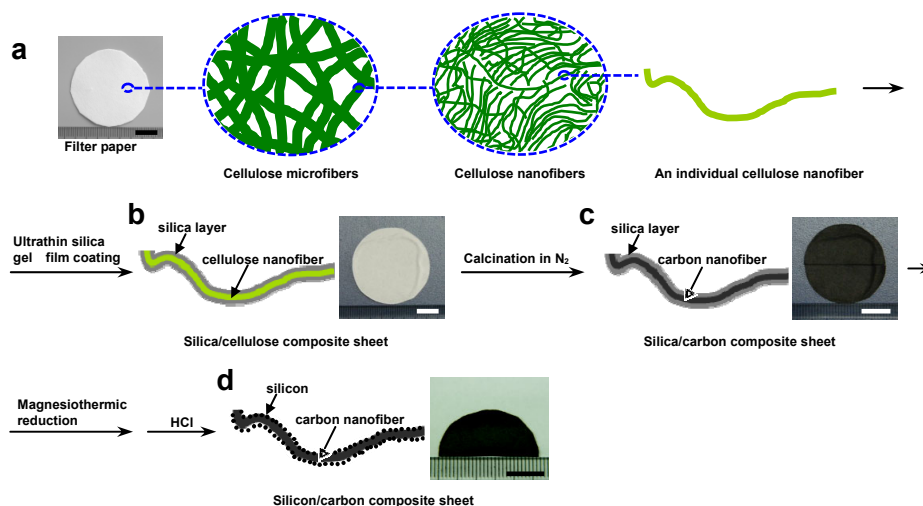
Mengya Wang, Dongling Jia, Jiao Li and Jianguo Huang*

Department of Chemistry, Zhejiang University, Hangzhou, Zhejiang 310027, China

E-mail: jghuang@zju.edu.cn

Fabrication of the silicon/carbon composite sheet. Cellulose is a poly- β -(1,4)-D-glucopyranose, the polymer chains assemble into microfibrils (diameters of 3–4 nm) and microfibril aggregates (namely nanofibers, diameters of tens to hundreds of nanometers), and further bundle to form a randomly cross-linked network of fibres (namely microfibers, diameters in the micrometer level and larger; Scheme S1-a). To deposit ultrathin silica gel films to coat each nanofiber of the filter paper, a piece of laboratory quantitative filter paper (diameter 5 cm) was placed in a suction filter funnel, prior to use, it was washed by suction filtration of ethanol and successively dried with air flow. Deposition of the silica films by the surface sol–gel process was carried out at about 60 °C using tetramethoxysilane (TMOS, Aldrich, 99%; 0.50 M in methanol) as the precursor. Thirty milliliters of TMOS solution (0.5 M in methanol) was added to the filter funnel, the first 10 mL of which was slowly suction-filtered through the filter paper, and the rest was left to stand for 15 min to ensure adsorption of silicon alkoxide on the cellulose nanofibre surfaces. The

remaining 20 mL TMOS solution afterwards suction filtered slowly through the filter paper, and immediately two 20 mL portions of methanol were filtered to remove the excessively adsorbed unreacted silicon alkoxide.



Scheme S1 Schematic illustration of the preparation process of the hierarchical silicon/carbon nanocomposite sheet derived from the natural cellulose substance (ordinary laboratory quantitative cellulose filter paper). (a) The macro- to nano-scale hierarchical structures of the filter paper. (b) Ultrathin silica gel layers were deposited to coat each cellulose nanofiber of the filter paper followed by carbonization of the resulting silica/cellulose composite sheet in nitrogen atmosphere. (c) The silica/carbon nanocomposite sheet obtained was applied with magnesiothermic reduction to give the silicon/carbon nanocomposite sheet (d). The photographs show the corresponding specimens; scale bars: 1 cm.

Then twenty milliliters of hot water (purified using a Milli-Q Advantage A10 system with resistivity higher than 18.2 MΩ cm) was added to the funnel and allowed to pass through the filter paper slowly within 10 min to promote hydrolysis of silicon alkoxide. The filter paper was finally dried with air flow to finish the deposition cycle.

Each cellulose nanofibre of the filter paper was thus coated with a silica gel layer with thickness of *ca.* 0.5–0.75 nm. The deposition cycle was repeated for a given number of times (namely 5, 10, 15 and 20 times) to give the silica/cellulose composite sheets with silica gel films of varied thickness coating on the cellulose nanofibers of the filter paper (Scheme S1-b) . The as-deposited silica/cellulose composite sheets were then subjected to calcination and carbonation in argon atmosphere at 600 °C for 6 h, resulting in the silica/carbon composite sheets (Scheme S1-c); the reduction of the silica component of which into silicon was thereafter achieved by a low-temperature magnesiothermic reduction process employing a home-made stainless steel autoclave. Magnesium granules (Aldrich, 98%) and the silica/carbon composite sheet (with 2.5:1 molar ratio of Mg and SiO₂) sheet were put separately in two steel boats, which were placed in the autoclave. The magnesiothermic reduction was performed in argon atmosphere at 750 °C for 3 h, the raw product was washed with 1 M HCl to remove the by-product magnesia to give the silicon/carbon composite sheet (Scheme S1-d).

Structure and morphology characterization. To prepare the specimens for the FE-SEM and TEM observations, a small piece of the corresponding sample was suspended in ethanol by ultrasonication for 20 s, the suspension was then dropped onto silicon wafer for SEM observation, or onto copper mesh for TEM observation, and the specimens were dried in air. FE-SEM images were obtained on a FEI Sirion-100 instrument with EDAX Genesis 4000 working at an accelerating voltage of 25.0 kV, and the specimens were sputtered with platinum to reduce charging; TEM micrographs were acquired on a Hitachi HT-7700 microscope operating at an

accelerating voltage of 100 kV; HR-TEM observations were performed on a FEI Tecnai F20 microscope operated at an acceleration voltage of 200 kV. XPS spectra were measured on a VG Escalab Mark II spectrophotometer equipped with an Mg K_{α} X-ray source at energy of 1253.6 eV, and the spectra were calibrated according to the C 1s peak at 284.6 eV. X-ray diffraction (XRD) measurements were conducted using a Philips X'Pert PRO diffractometer with a Cu K_{α} ($\lambda = 0.15418$ nm) radiation source. Raman spectra were acquired using a Jobin Yvon LabRam HR UV Raman spectrometer operating at the excitation wavelength of 514 nm.

Electrochemical characterization. Standard CR2025 type coin cells were assembled in an argon-filled glovebox with oxygen and water contents less than 0.1 ppm, using the silicon/carbon composite sheet ($\sim 6 \times 6$ mm², weights ~ 1.3 mg) directly as the working electrode with Celgard 2300 film as separator and lithium-foil as counter/reference electrode. The electrolyte was 1.0 M LiPF₆ dissolved in a mixture of ethylene carbonate (EC), dimethyl carbonate (DMC) and ethyl methyl carbonate (EMC) with a volume ration of 1:1:1. Cyclic voltammetry (CV) was carried out using a CHI760D electrochemical workstation (CH Instruments, Inc., China) with a scan rate of 0.1 mV s⁻¹ between 0.01 and 3 V. The battery performances were evaluated using a Neware battery testing system (Neware Technology Co., Ltd., Shenzhen, China) at room temperature. Galvanostatic charge/discharge capacities were measured by cycling the half cells in the voltage range of 0.01–3 V *versus* Li/Li⁺. The specific capacity is based on the mass or area of the silicon/carbon composite electrode.

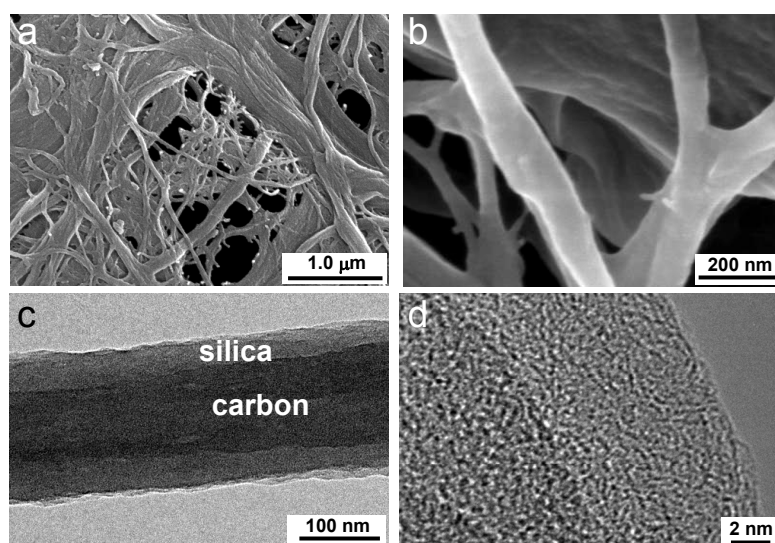


Fig. S1 The silica/carbon nanocomposite sheet obtained by carbonization of the as-prepared silica/cellulose composite sheet under nitrogen atmosphere, deposition of silica thin films was repeated 20 times for the sample. (a) FE-SEM image of the silica/carbon nanocomposite sheet. (b) A higher magnification FE-SEM image of the sample. (c) TEM image of an individual silica/carbon nanocomposite fiber. (d) HR-TEM micrograph of the nanocomposite fiber.

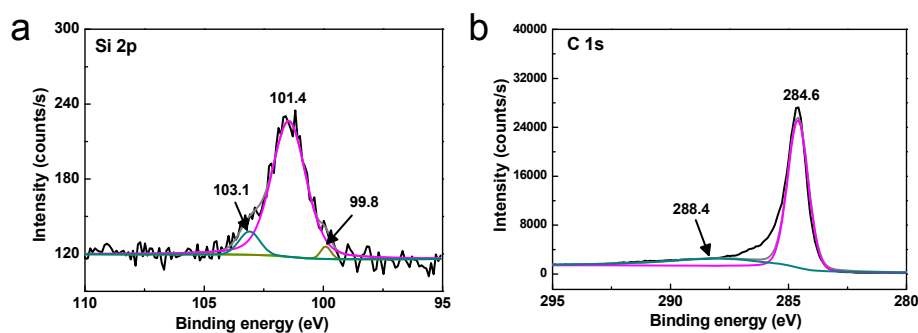


Fig. S2 XPS spectra (a, Si 2p region; b, C 1s region) of the silicon/carbon nanocomposite sheet, deposition of silica thin films was repeated 20 times for the sample.

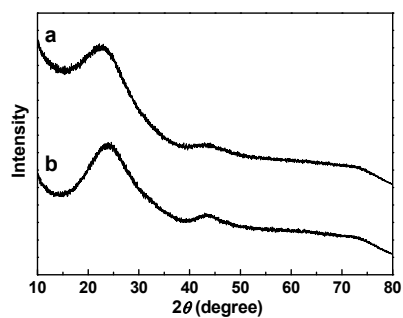


Fig. S3 XRD patterns of the silica/carbon (a) and silicon/carbon (b) nanocomposite sheets, deposition of silica thin films was repeated 20 times to prepare the samples.

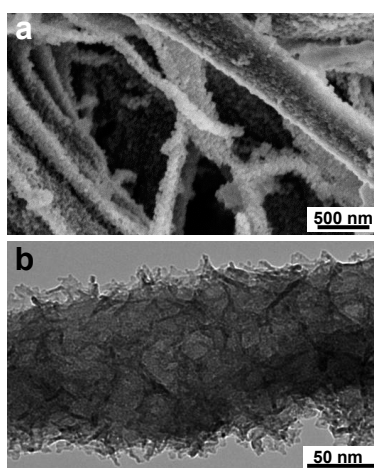


Fig. S4 Electron microscope images of the silicon/carbon nanocomposite sheet anode after 50 cycles charge/discharge processes. (a) FE-SEM image shows the porous network structure maintained. (b) TEM image of an individual silicon/carbon nanocomposite fiber.